

FUSE OBSERVATIONS OF THE LOW-REDSHIFT Ly β FOREST

J. MICHAEL SHULL^{1,2}, MARK L. GIROUX¹, STEVEN V. PENTON¹, JASON
 TUMLINSON¹, JOHN T. STOCKE¹, EDWARD B. JENKINS³, H. WARREN MOOS⁴,
 WILLIAM R. OEGERLE⁴, BLAIR D. SAVAGE⁵, KENNETH R. SEMBACH⁴, DONALD G.
 YORK⁶, JAMES C. GREEN¹, AND BRUCE E. WOODGATE⁷

Draft version November 19, 2018

ABSTRACT

We describe a moderate-resolution (20–25 km s^{−1}) FUSE study of the low-redshift intergalactic medium. We report on studies of 7 extragalactic sightlines and 12 Ly β absorbers that correspond to Ly α lines detected by HST/GHRS and STIS. These absorbers appear to contain a significant fraction of the low- z baryons and were a major discovery of the HST spectrographs. Using FUSE data, with 40 mÅ (4 σ) Ly β detection limits, we have employed the equivalent width ratio of Ly β /Ly α , and occasionally higher Lyman lines, to determine the doppler parameter, b , and accurate column densities, N_{HI} , for moderately saturated lines. We detect Ly β absorption corresponding to all Ly α lines with $W_{\lambda} \geq 200$ mÅ. The Ly β /Ly α ratios yield a preliminary distribution function of doppler parameters, with mean $\langle b \rangle = 31.4 \pm 7.4$ km s^{−1} and median 28 km s^{−1}, comparable to values at redshifts $z = 2.0$ – 2.5 . If thermal, these b -values correspond to $T_{\text{HI}} \approx 50,000$ K, although the inferred doppler parameters are considerably less than the widths derived from Ly α profile fitting, $\langle b/b_{\text{width}} \rangle = 0.52$. The typical increase in column density over that derived from profile fitting is $\Delta \log N_{\text{HI}} = 0.3$ but ranges up to 1.0 dex. Our data suggest that the low- z Ly α absorbers contain sizable non-thermal motions or velocity components in the line profile, perhaps arising from cosmological expansion and infall.

Subject headings: intergalactic medium — quasars: absorption lines — ultraviolet: galaxies

1. INTRODUCTION

Since the discovery of the high-redshift Ly α forest over 25 years ago, these abundant absorption features in the spectra of QSOs have been used as evolutionary probes of the intergalactic medium (IGM), galactic halos, large-scale structure, and chemical evolution. The *Hubble Space Telescope* (HST/FOS) Key Project on QSO absorption systems found that Ly α absorbers persist to low redshift in surprisingly large numbers (Bahcall et al. 1991; Morris et al. 1991; Jannuzi et al. 1998; Weymann et al. 1998). In this paper, we assume that the Ly α (and Ly β) lines are intergalactic. Richards et al. (1999) discuss the possibility that some C IV absorption systems could be intrinsic to the AGN or ejected at relativistic velocities.

The Colorado group has used HST to conduct a major survey of Ly α absorbers at low redshift ($z \leq 0.07$) along 15 AGN sightlines, using the moderate-resolution (19 km s^{−1}) GHRS spectrograph (Stocke et al. 1995; Shull, Stocke, & Penton 1996; Penton et al. 2000a,b). Additional moderate-resolution HST/STIS data along 13 sightlines were taken during HST cycle 7. These observations measured Ly α absorbers down to equivalent widths of 10–20 mÅ and determined distributions of the low- z Ly α absorbers in H I column density for $12.3 < \log N_{\text{HI}} < 14.0$ and in line width for $15 < b_{\text{width}} < 100$ km s^{−1} (Penton et al. 2000b).

The distribution function, $dN/dN_{\text{HI}} \propto N_{\text{HI}}^{-1.80 \pm 0.05}$, together with photoionization corrections suggest (Shull et al. 1999a) that the low- z Ly α forest may contain a significant fraction of the baryons predicted by nucleosynthesis models of D/H (Burles & Tytler 1998).

However, a precise baryon census in the low- z IGM requires measurements of the true doppler parameter, b , to obtain accurate column densities in saturated Ly α lines with $\log N_{\text{HI}} \geq 13.5$. Measurements of Ly β or higher Lyman lines are needed to constrain the degree of saturation through a curve-of-growth (COG) analysis. Indeed, recent ORFEUS studies (Hurwitz et al. 1998) of Ly β /Ly α ratios in two absorbers toward 3C 373 suggest that b is less than the line width determined from Ly α profile fitting.

With the goal of characterizing the distribution of b -values and measuring accurate H I columns, we conducted a FUSE mini-survey of Ly β absorbers toward 7 AGN with well-known Ly α lines. The FUSE mission and its capabilities are described by Moos et al. (2000) and Sahnou et al. (2000). In § 2 we describe our FUSE Ly β observations. We also compare simple COG (Ly β /Ly α) estimates of b with single-component fits to (HST) Ly α lines to understand the kinematic structure of the low- z absorbers. In § 3 we present our conclusions and give directions for future work on the IGM baryon content, line kinematics, and temperature.

¹CASA and Dept. of Astrophysical and Planetary Sciences, University of Colorado, Boulder, CO 80309

²Also at JILA, University of Colorado and National Institute of Standards and Technology

³Dept. of Astrophysical Sciences, Princeton University, Princeton, NJ 08544

⁴Dept. of Physics & Astronomy, Johns Hopkins University, Baltimore, MD 21218

⁵Dept. of Astronomy, University of Wisconsin, Madison, WI 53706

⁶Dept. of Astronomy & Astrophysics, Univ. of Chicago, Chicago, IL 60637

⁷NASA Goddard Space Flight Center, Greenbelt, MD 20771

2. FUSE OBSERVATIONS AND DATA ANALYSIS

Our observations were obtained with the FUSE satellite from 1999 September to November during the commissioning phase. Because the initial FUSE observations were taken with relatively long durations (16–49 ksec) we were able to obtain reasonable signal-to-noise ratios ($S/N \approx 15\text{--}20$) in the LiF channels. The SiC channels had lower S/N and were not available for all targets. The spectral resolution was generally $20\text{--}25 \text{ km s}^{-1}$, based on an analysis of narrow interstellar lines of H_2 , Ar I, and Fe II in our H_2 mini-survey (Shull et al. 2000).

Our FUSE $\text{Ly}\beta$ mini-survey consisted of 7 AGN chosen from targets for which the Colorado group had previously obtained HST spectra with GHRS/G160M or STIS/E140M. Our three GHRS targets and full line lists are: H1821+643 (Savage, Sembach, & Lu 1995; Tripp, Lu, & Savage 1998; Penton et al. 2000a), ESO 141-G55 (Sembach, Savage, & Hurwitz 1999; Penton et al. 2000a), and PKS 2155-304 (Shull et al. 1998; Penton et al. 2000a). Data on our four STIS targets (Mrk 876, PG 0804+761, VII Zw 118, and Ton S180) will be published separately.

From these 7 targets, we chose 12 strong $\text{Ly}\alpha$ absorbers with rest-frame equivalent widths $W_\lambda > 200 \text{ m}\text{\AA}$ and relatively simple line profiles. Each of the $\text{Ly}\alpha$ lines had a detectable $\text{Ly}\beta$ counterpart, and in several cases we detected higher Lyman series lines. Figure 1 shows three examples: the 5512 km s^{-1} $\text{Ly}\beta$ absorber toward Ton S180; the $z = 0.225$ $\text{Ly}\delta$ absorber toward H1821+643; and the $10,463 \text{ km s}^{-1}$ $\text{Ly}\beta$ absorber toward ESO 141-G55. Although PKS 2155-304 contains several strong $\text{Ly}\alpha$ lines near $cz = 17,000 \text{ km s}^{-1}$, their line blending is sufficiently complex that we did not include them in the survey. For the 12 chosen lines, we measured equivalent widths by gaussian profile fitting, using standard FUSE pipeline software. Assuming a single-component curve of growth, we used the concordance of the $\text{Ly}\beta/\text{Ly}\alpha$ ratios (or higher Lyman lines) to derive b and N_{HI} . After minimizing the χ^2 of our fits to N_{HI} and b , we constructed $\Delta\chi^2$ contours to define confidence regions for these inferred quantities. The error bars on N_{HI} and b represent single-parameter 68% confidence intervals for each component and assume that the true line shape is well represented by a single-component, doppler-broadened line.

If $\text{Ly}\alpha$ and $\text{Ly}\beta$ are unsaturated, their equivalent widths are $W_\lambda^{\text{Ly}\alpha} = (54.5 \text{ m}\text{\AA})N_{13}$ and $W_\lambda^{\text{Ly}\beta} = (7.37 \text{ m}\text{\AA})N_{13}$, where $N_{\text{HI}} = (10^{13} \text{ cm}^{-2})N_{13}$. Thus, weak absorbers should have a ratio $\text{Ly}\beta/\text{Ly}\alpha = 0.135$, and saturation gradually increases this ratio towards 1. Our typical FUSE $\text{Ly}\beta$ detection limit of $40 \text{ m}\text{\AA}$ (4σ) corresponds to $\log N_{\text{HI}} \geq 13.73$. Our success in detecting $\text{Ly}\beta$ for all $\text{Ly}\alpha$ lines with $W_\lambda > 200 \text{ m}\text{\AA}$ is consistent with the relative line strengths.

Table 1 lists the 12 lines in our survey, together with $\text{Ly}\alpha$ velocities (cz) and line widths (b_{width}) derived from instrumentally corrected gaussian fits to the GHRS or STIS $\text{Ly}\alpha$ profiles. Here, $b_{\text{width}} = 2^{1/2}\sigma_{\text{gauss}}$, and b and N_{HI} are derived from the COG. Figures 2 and 3 show COG concordance plots for two absorbers in Fig. 1. Not including the broad, blended line at $16,203 \text{ km s}^{-1}$ toward PKS 2155-304, the FUSE distribution has mean $\langle b \rangle = 31.4 \pm 7.4 \text{ km s}^{-1}$ and median 28 km s^{-1} , comparable to the values, $\langle b \rangle = 27.5 \pm 1.3 \text{ km s}^{-1}$ and me-

dian 26.4 km s^{-1} , measured in the $z = 2.0\text{--}2.5$ $\text{Ly}\alpha$ forest (Rauch et al. 1993). If thermal, these b -values correspond to $T_{\text{HI}} = m_H b^2 / 2k \approx 50,000 \text{ K}$, a temperature higher than values predicted from models of low-metallicity $\text{Ly}\alpha$ clouds (Donahue & Shull 1991), heated and photoionized by the AGN metagalactic background. These models predict temperatures and doppler parameters, conveniently approximated by $T = (24,300 \text{ K})(U/0.01)^{0.152}$ and $b = (20 \text{ km s}^{-1})(U/0.01)^{0.076}$. The doppler parameter scales weakly with the photoionization parameter $U = n_\gamma/n_H \approx (0.005)J_{-23}(10^{-5} \text{ cm}^{-3}/n_H)$. Here, U is the ratio of ionizing photons to hydrogen nuclei for a specific intensity $J_0 = (10^{-23} \text{ ergs s}^{-1} \text{ cm}^{-2} \text{ sr}^{-1} \text{ Hz}^{-1})J_{-23}$.

The doppler parameters inferred from $\text{Ly}\beta/\text{Ly}\alpha$ are considerably less than widths derived from $\text{Ly}\alpha$ profile-fitting. The statistical average, $\langle b/b_{\text{width}} \rangle = 0.52$, suggests that the $\text{Ly}\alpha$ and $\text{Ly}\beta$ line profiles are more complex than single-component, doppler-broadened gaussians. The widths of individual components must be less than the COG-inferred b -values, a general principle exemplified by the special case where N identical, well-separated gaussians behave as a single one with a dispersion equal to Nb . For each ensemble of components, the total column density derived from $\text{Ly}\alpha$ and $\text{Ly}\beta$ might be larger than the true value, but not by a large factor (Jenkins 1986).

The $\text{Ly}\alpha$ absorbers could be broadened by cosmological expansion, $\Delta v = (19.5 \text{ km s}^{-1})(\Delta r/300 \text{ kpc})h_{65}$, across spatially extended H I absorbers, as seen in numerical simulations (Weinberg, Katz, & Hernquist 1998). The profiles could also be blends of velocity components arising from clumps of gas falling into dark-matter potential wells. If these clumps are sufficiently massive to be gravitationally bound, the velocity components may represent small-scale power at $\Delta v < 100 \text{ km s}^{-1}$ in the cosmological spectrum of density fluctuations. We have seen spectral evidence for such velocity components in the low- z $\text{Ly}\alpha$ absorbers studied by HST/GHRS and STIS at 19 km s^{-1} resolution and in their two-point correlation function, $\xi(\Delta v)$ (Penton et al. 2000b,c). We have also verified, through optical and 21-cm imaging, that some $\text{Ly}\alpha$ absorbers arise within small groups (van Gorkom et al. 1996; Shull et al. 1998).

With better statistics on the $\text{Ly}\alpha$ and $\text{Ly}\beta$ line widths and doppler parameters, we should be able to constrain the kinematics of the absorber profiles. A critical issue is whether cosmological expansion or velocity components are the dominant contributor to line broadening. Recent numerical simulations of the low- z $\text{Ly}\alpha$ forest (Davé et al. 1999) suggest that both effects are important.

3. CONCLUSIONS AND DISCUSSION

First and foremost, FUSE has identified the low-redshift $\text{Ly}\beta$ forest. Lines between 1216 \AA and $(1216 \text{ \AA})(1 + z_{\text{em}})$ with no clear identification are often labeled as $\text{Ly}\alpha$. The FUSE detection of their $\text{Ly}\beta$ counterparts makes these identifications conclusive. We have used the COG concordance of $\text{Ly}\beta/\text{Ly}\alpha$ equivalent widths, and occasionally higher Lyman lines, to derive reliable values of b and N_{HI} for the stronger, saturated lines ($W_\lambda > 200 \text{ m}\text{\AA}$). Our major findings are: (1) The doppler parameters from single-component COG fits to $\text{Ly}\beta/\text{Ly}\alpha$ equivalent widths are considerably less than those derived from line profile fitting, with $\langle b/b_{\text{width}} \rangle = 0.52$; (2) We find $\langle b \rangle = 31.4 \pm 7.4$

km s⁻¹ (median 28 km s⁻¹), similar to values at redshifts $z = 2.0$ – 2.5 ; (3) Although these b -values correspond to $T_{\text{HI}} \approx 50,000$ K, the low- z absorbers may contain non-thermal motions or line broadening from cosmological expansion and infall.

Over its lifetime, FUSE will observe many AGN sight-lines for the O VI, D/H, and AGN projects. This will produce a large survey of Ly β absorbers at $z < 0.155$ that we can use to characterize the distributions in b and N_{HI} in the low-redshift Ly β forest. The distribution function, $f(b)$, can be used to derive the IGM temperature distribution and infer its equation of state (Schaye et al. 1999; Ricotti, Gnedin, & Shull 2000). With high-S/N data and a flux-limited sample, we can search for the hot baryons predicted by cosmological simulations (Cen & Ostriker 1999a). These absorbers should appear in the high- b tail of the distribution as broad, shallow absorbers.

Because Ly α lines with $W_\lambda > 130$ mÅ ($\log N_{\text{HI}} > 13.5$) appear to be saturated (Penton et al. 2000b), HST alone cannot provide accurate column densities for the strong Ly α absorbers that probably dominate the baryon content and opacity of the low- z IGM. For lines in which b is well determined, $\log N_{\text{HI}}$ typically increases by 0.3 dex, and up to 1 dex, compared to Ly α profile fitting. This increase, which is greatest in the most saturated Ly α lines, means that an even larger fraction of baryons may be found in

the low- z Ly α forest.

A full Ly β survey will also provide a sample of high- N_{HI} absorbers which can be used to estimate the level of metallicity in the low- z IGM (Shull et al. 1998; Cen & Ostriker 1999b). As an illustration, we constructed simple photoionization models using CLOUDY (Ferland 1996) that assume a specific ionizing intensity at 13.6 eV of $J_\nu = 10^{-23}$ ergs cm⁻² s⁻¹ sr⁻¹ Hz⁻¹ (Shull et al. 1999b) with $J_\nu \propto \nu^{-1.8}$ and column density $\log N_{\text{HI}} = 15$. For total hydrogen densities (cm⁻³) of $\log n_H = (-3, -4, -5)$, a 20 mÅ measurement of C III $\lambda 977$ implies $Z/Z_\odot = (0.3, 0.15, 0.01)$. For $\log n_H = (-5, -6)$, a 20 mÅ measurement of O VI $\lambda 1032$ implies $Z/Z_\odot = (0.015, 0.006)$. Observations of C III $\lambda 977$ will be especially useful, because they can be compared with C II and/or C IV to obtain reliable ionization corrections.

This work is based on FUSE Team data obtained for the Guaranteed Time Team by the NASA-CNES-CSA FUSE mission operated by Johns Hopkins University. Financial support to U. S. participants has been provided by NASA contract NAS5-32985. The Colorado group also acknowledges support from astrophysical theory grants from NASA (NAG5-7262) and NSF (AST96-17073), the HST/COS project (NAS5-98043), and STScI grant GO-0653.01-95A which supported the Ly α data analysis.

REFERENCES

- Bahcall, J. N., Jannuzi, B. T., Schneider, B. P., Hartig, G. F., Bohlin, R., & Junkkarinen, V. 1991, ApJ, 377, L5
 Burles, S., & Tytler, D. 1998, ApJ, 507, 732
 Cen, R., & Ostriker, J. P. 1999a, ApJ, 514, 1
 Cen, R., & Ostriker, J. P. 1999b, ApJ, 519, L109
 Davé, R., Hernquist, L., Katz, N., & Weinberg, D. 1999, ApJ, 511, 521
 Donahue, M., & Shull, J. M. 1991, ApJ, 383, 511
 Ferland, G. J. 1996, HAZY, A Brief Introduction To Cloudy (Univ. Kentucky Phys. & Astron. Dept. Internal Rept.)
 Hurwitz, M., et al. 1998, ApJ, 500, L61
 Jannuzi, B. T., et al. 1998, ApJS, 118, 1
 Jenkins, E. B. 1986, ApJ, 304, 739
 Moos, H. W., et al. 2000, ApJ, this issue
 Morris, S. L., Weymann, R. J., Savage, B. D., & Gilliland, R. L. 1991, ApJ, 377, L21
 Penton, S. V., Stocke, J. T., & Shull, J. M. 2000a, ApJ, in press (astro-ph/9911117)
 Penton, S. V., Shull, J. M., & Stocke, J. T. 2000b, ApJ, in press (astro-ph/9911128)
 Penton, S. V., Stocke, J. T., & Shull, J. M. 2000c, BAAS, 31, 1387
 Rauch, M., Carswell, R. F., Webb, J. K., & Weymann, R. J. 1993, MNRAS, 260, 589
 Richards, G. T., York, D. G., Yanny, B., Kollgaard, R. I., Laurent-Muehleisen, S. A., & Vanden Berk, D. E. 1999, ApJ, 513, 576
 Ricotti, M., Gnedin, N. Y., & Shull, J. M. 2000, ApJ, 534, in press (astro-ph/9906413)
 Sahnou, D. et al. 2000, ApJ, this issue
 Savage, B. D., Sembach, K. R., & Lu, L. 1995, ApJ, 449, 145
 Schaye, J., Theuns, T., Leonard, A., & Efstathiou, G. 1999, MNRAS, 310, 57
 Sembach, K. R., Savage, B. D., & Hurwitz, M. 1999, ApJ, 524, 98
 Shull, J. M., Stocke, J. T., & Penton, S. V. 1996, AJ, 111, 72
 Shull, J. M., Penton, S. V., Stocke, J. T., Giroux, M. L., van Gorkom, J. H., Lee, Y.-H., & Carilli, C. 1998, AJ, 116, 2094
 Shull, J. M., Penton, S. V., & Stocke, J. T. 1999a, PASA, Vol. 16, No. 1, 95
 Shull, J. M., Roberts, D., Giroux, M. L., Penton, S. V., & Fardal, M. A. 1999b, AJ, 118, 1450
 Shull, J. M., Tumlinson, J., et al. 2000, ApJ, this issue
 Stocke, J. T., Shull, J. M., Penton, S. V., Donahue, M., & Carilli, C. 1995, ApJ, 451, 24
 Tripp, T., Lu, L., & Savage, B. D. 1998, ApJ, 508, 200
 Weinberg, D. H., Katz, N., & Hernquist, L. 1998, in Origins, ed. C. E. Woodward, J. M. Shull, & H. A. Thronson, ASP Conference Series, Vol. 148, 21
 Weymann, R. J., et al. 1998, ApJ, 506, 1
 van Gorkom, J. H., Carilli, C. L., Stocke, J. T., Perlman, E. S., & Shull, J. M. 1996, AJ, 112, 1397

TABLE 1
FUSE LY β LINES¹

AGN	t_{exp} (ksec)	Ly α Velocity (km s ⁻¹)	$W_{\lambda}(\text{Ly}\alpha)$ (mÅ)	$W_{\lambda}(\text{Ly}\beta)$ (mÅ)	$\log N_{HI}^{\text{Ly}\alpha}$ (cm ⁻²)	$b_{\text{width}}^{\text{Ly}\alpha}$ (km s ⁻¹)	$\log N_{HI}$ (cm ⁻²)	b (km s ⁻¹)
ESO 141-G55	35.8	10,463 ²	354±11	164±40	14.06±0.03	49±3	14.57 ^{+0.25} _{-0.23}	27 ⁺⁵ ₋₃
H1821+643	48.8	7342	298±20	90±30	13.93 ^{+0.05} _{-0.04}	49±3	14.23 ^{+0.19} _{-0.18}	27 ⁺⁸ ₋₄
		63,933	483±18	155±18	14.31 ^{+0.08} _{-0.06}	49±2	14.43 ^{+0.07} _{-0.06}	43 ⁺³ ₋₃
		67,420 ³	739±22	511±21	14.41±0.04	87±2	15.46 ^{+0.06} _{-0.05}	45 ⁺² ₋₁
Mrk 876	45.9	958	324±52	170±40	13.89±0.11	72±8	14.42 ^{+0.09} _{-0.13}	26 ⁺⁶ ₋₅
PG 0804+761	39.6	5565	329±18	90±30	13.94 ^{+0.03} _{-0.04}	57±2	14.18 ^{+0.17} _{-0.24}	32 ⁺²⁶ ₋₅
VII Zw 118	26.0	2463	355±35	110±50	14.01 ^{+0.13} _{-0.10}	54±8	14.28 ^{+0.27} _{-0.34}	32 ⁺⁴⁹ ₋₇
PKS 2155-304	37.1	5119	218±20	40±20	13.68 ^{+0.04} _{-0.05}	82±5	13.76 ^{+0.22} _{-0.13}	41 ^{+∞} ₋₂₀
		16,203	346±23	40±20	13.96±0.05	60±3	13.88 ^{+0.09} _{-0.03}	98 ^{+∞} ₋₄₄
TON S180	16.5	5512	271±16	71±15	13.82±0.04	58±2	14.05 ^{+0.12} _{-0.12}	28 ⁺⁹ ₋₄
		7025	236±17	65±40	13.72±0.04	67±3	14.03 ^{+0.32} _{-0.35}	23 ^{+∞} ₋₅
		13,688	229±17	55±15	13.72±0.04	63±3	13.94 ^{+0.13} _{-0.18}	25 ⁺²² ₋₅

¹Columns, left to right: (1) AGN sightline; (2) FUSE exposure time; (3) recession velocity (cz) relative to LSR; (4, 5) rest-frame Ly α and Ly β equivalent widths with 1σ uncertainties; (6) H I column density from fit of single-component, doppler-broadened and instrumentally broadened Ly α profile; (7) instrumentally corrected Ly α line width and 1σ uncertainty; (8, 9) H I column density and doppler parameter, based on Ly β /Ly α equivalent width ratio (exceptions below). Uncertainties represent 68% confidence interval. FUSE observations of higher Lyman series lines were also used in analysis of the following: H1821+643, $cz = 7344 \text{ kms}^{-1}$, $W_{\lambda}(\text{Ly}\gamma) = 57 \pm 30 \text{ mÅ}$; H1821+643, $cz = 63933 \text{ kms}^{-1}$, $W_{\lambda}(\text{Ly}\gamma) = 62 \pm 25 \text{ mÅ}$; H1821+643, $cz = 67420 \text{ kms}^{-1}$, $W_{\lambda}(\text{Ly}\delta) = 212 \pm 25 \text{ mÅ}$, $W_{\lambda}(\text{Ly}\epsilon) = 139 \pm 25 \text{ mÅ}$; Mrk 876, $cz = 958 \text{ kms}^{-1}$, $W_{\lambda}(\text{Ly}\gamma) = 40 \pm 20 \text{ mÅ}$.

²Associated Ly α absorber; Ly γ indicates two velocity components, separated by 70 km s^{-1}

³Ly δ (Fig. 2) indicates two velocity components, separated by 70 km s^{-1}

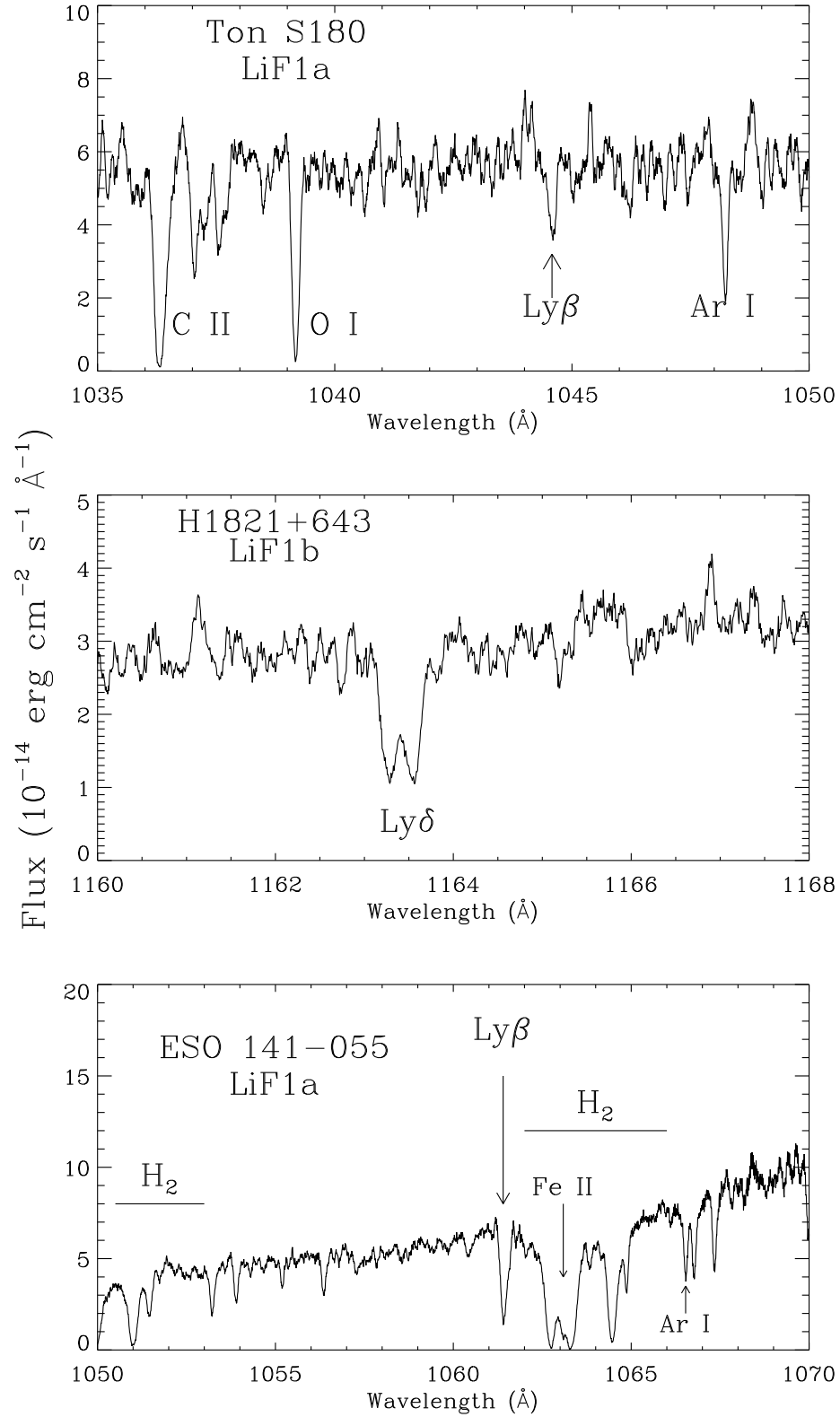


FIG. 1.— FUSE spectra of three absorbers toward targets Ton S180 (Ly β in 5512 km s $^{-1}$ absorber), H1821+643 (Ly δ in $z = 0.225$ absorber), and ESO 141-G55 (Ly β in 10,463 km s $^{-1}$ absorber). The H1821+643 Ly δ absorber shows two components separated by 70 km s $^{-1}$.

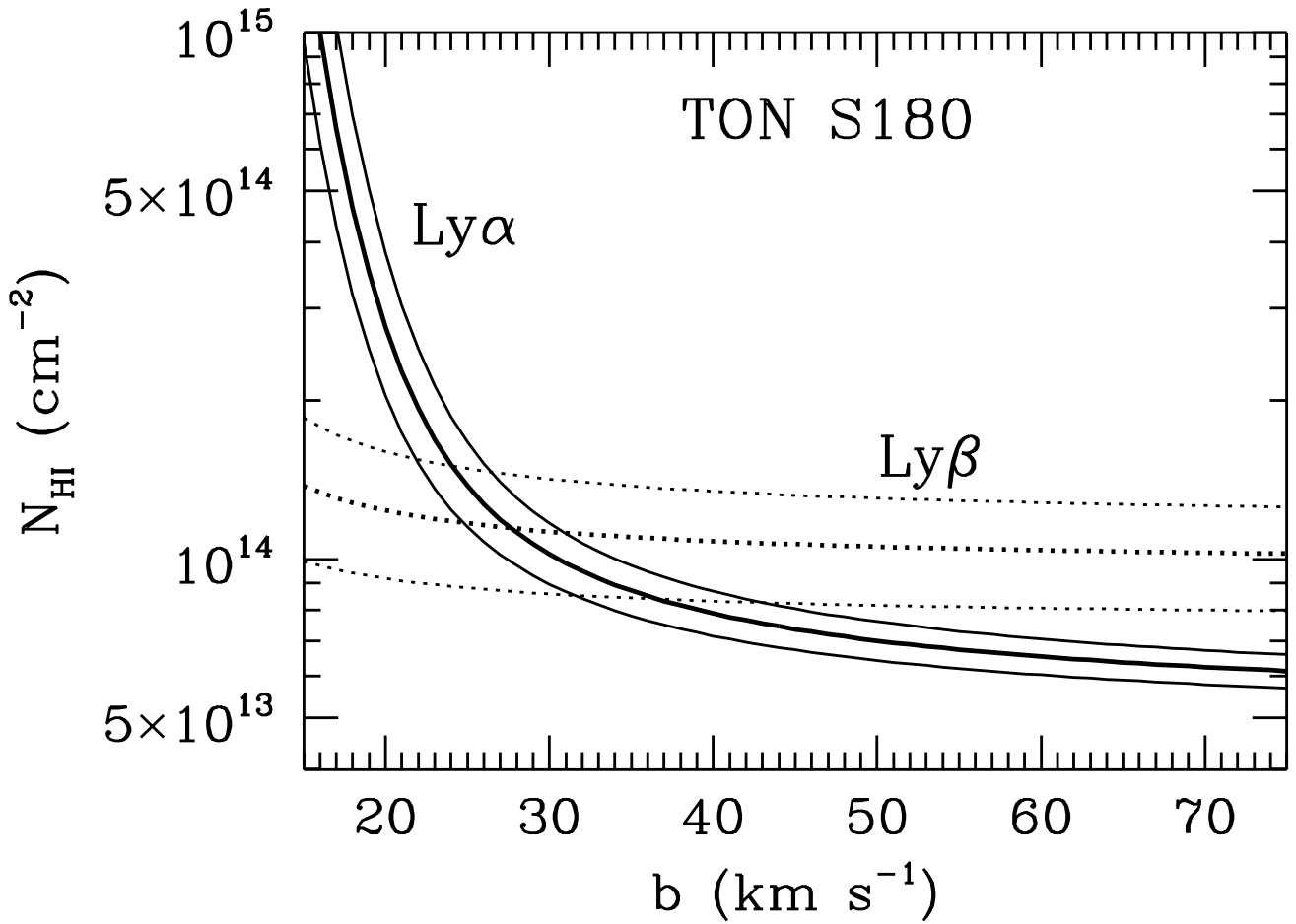


FIG. 2.— COG concordance plot in b and N_{HI} for $\text{Ly}\alpha$ ($271 \pm 16 \text{ m}\text{\AA}$) and $\text{Ly}\beta$ ($71 \pm 15 \text{ m}\text{\AA}$) at $cz = 5512 \text{ km s}^{-1}$ toward Ton S180. Three curves for each line show single-component, doppler-broadened COG fits to equivalent widths ($\pm 1\sigma$ errors).

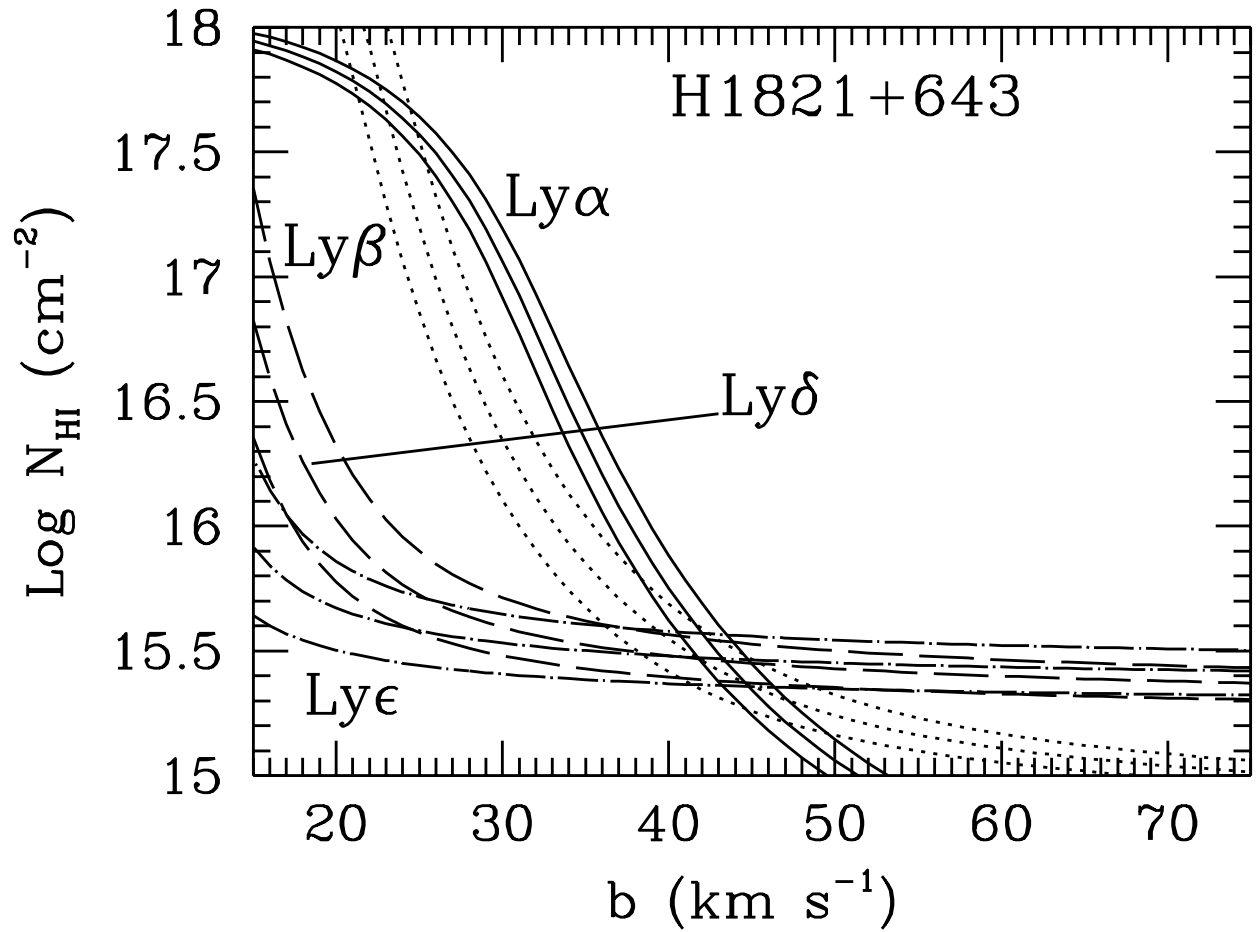


FIG. 3.— COG concordance plot (see Fig. 2) for absorber at $z = 0.225$ toward H1821+643. The curves of growth are based on rest-frame equivalent widths for Ly α (739 ± 22 mÅ) and Ly β (511 ± 21 mÅ) from HST/GHRS/G160M and for Ly δ (212 ± 25 mÅ) and Ly ϵ (139 ± 25 mÅ) from FUSE.